

Radiation Responses of Human Mesenchymal Stem Cells Derived From Different Sources

Dose-Response:
An International Journal
October-December 2019:1-9
© The Author(s) 2019
Article reuse guidelines:
sagepub.com/journals-permissions
DOI: 10.1177/1559325819893210
journals.sagepub.com/home/dos



Ningning He¹ , Changyan Xiao¹, Yuxiao Sun¹ , Yan Wang¹, Liqing Du¹, Yu Feng², Yang Liu¹, Qin Wang¹, Kaihua Ji¹, Jinhan Wang¹, Manman Zhang¹, Chang Xu¹, and Qiang Liu¹

Abstract

Mesenchymal stem cells (MSCs) derived from different tissues may aid in the regeneration of radiation-induced organ lesions; however, the radiation responses of human MSCs from different sources are unknown. In our study, a comparison of the results from cell proliferation, apoptosis, cell cycle, DNA damage, and DNA repair assays consistently showed that MSCs derived from adipose tissue possess a significantly stronger radiation resistance capacity than MSCs derived from umbilical cord and gingival, which is accompanied by a higher level of phosphorylated signal transducer and activator of transcription 3 (Stat3) expression. This reminds us Stat3 could be a potential biomarker of radiation resistance. These findings provide a better understanding of radiation-induced biologic responses in MSCs and may lead to the development of better strategies for stem cell treatment and cancer therapy.

Keywords

mesenchymal stem cells (MSCs), ionizing radiation, radiation resistance, biomarker

Introduction

Mesenchymal stem cells (MSCs) are a type of stem cell with multipotent properties that have been used extensively in regenerative medicine. In recent years, MSCs have exerted potential therapeutic effects on various clinical conditions, including immune diseases, wound healing, Alzheimer disease, and heart disease.¹⁻⁴ Mesenchymal stem cells may aid in the regeneration of ionizing radiation (IR)-induced tissue damage. Preclinical studies have confirmed the potential of MSCs to migrate into irradiation-induced lesion sites and support the regeneration of functional tissues.^{5,6} In addition, these cells also display a superior radiation resistance capacity in vitro and in vivo.^{7,8} Therefore, MSCs may be a promising anti-radiation therapy for clinical applications.

Radiation therapy is a highly efficient therapeutic method for the treatment of many cancers that potentially damage healthy tissues. In radiation oncology applications, MSC therapy is a rapidly growing domain of cell therapy for radiation-induced injury to normal tissues⁹ and has produced a significant restoration and improvement in intestinal injuries induced by IR.¹⁰⁻¹² However, the influence of IR on cellular survival and the functional aspects of MSCs from different origins remains unknown.

Mesenchymal stem cells with a strong anti-radiation capacity should be chosen before clinical application to obtain better therapeutic effects. In this study, 3 types of MSCs, adipose-derived MSCs (Ad-MSCs), umbilical cord MSCs (UC-MSCs), and gingival MSCs (G-MSCs), were utilized to compare their anti-radiation activities after exposure to relatively low and high doses of gamma rays. Cell proliferation, apoptosis, cell cycle, DNA damage, and DNA repair assays were conducted in

¹ Tianjin Key Laboratory of Radiation Medicine and Molecular Nuclear Medicine, Department of Radiobiology, Institute of Radiation Medicine of Chinese Academy of Medical Science and Peking Union Medical College, Tianjin, China

² Department of Respiratory, Tianjin people's Hospital, Tianjin, China

Received 14 July 2019; received revised 05 November 2019; accepted 06 November 2019

Corresponding Authors:

Chang Xu and Qiang Liu, Institute of Radiation Medicine, Chinese Academy of Medical Sciences and Peking Union Medical College, 238 Baidi Road, Nankai District, Tianjin 300192, China.

Emails: xuchang@irm-cams.ac.cn; liuqiang@irm-cams.ac.cn



the study. In addition, the expression of stat3 and its downstream genes was analyzed before and after exposure to IR to assess the potential mechanism regulating gene expression that underlies the radiation response of MSCs.

Materials and Methods

Cell Culture

Three types of MSCs, including Ad-MSCs (purchased from ATCC, Manassas, Virginia), UC-MSCs (isolated and cultured as described previously¹³), and G-MSCs (a gift from Beijing Taisheng Technology Co, Ltd, China) were used. They were cultured in Dulbecco modified Eagle medium (DMEM)/F12 supplemented with 10% fetal bovine serum (Gibco, Carlsbad, California), 100 U/mL penicillin/100 µg/mL streptomycin, and 1% l-glutamine (Gibco) and maintained in a humidified incubator with a 5% CO₂ atmosphere at 37°C.

Cell Proliferation Assay

Mesenchymal stem cells (3×10^4) were seeded in 12-well plates. The next day, cells were treated with 4- and 10-Gy irradiation. Cells were counted in 4 days after radiation. The relative proliferation result was obtained using the formula: [the cell number of the fourth day]/[the cell number of the first day].

Cell Irradiation

A Cs-137 (Gammacell-40) irradiator was purchased from Atomic Energy Co (Atomic Energy of Canadian Inc, Mississauga, Ontario, Canada). Cell or animal samples were placed in the center of the irradiation chamber and exposed to radiation at a dose rate of 1.02 Gy/min.

Cell Differentiation Assay

Cells were plated in 6-well plates and left to attach before being irradiated with 4 and 10 Gy. At 24 hours after treatment, differentiation medium was added to each well, and the cells were grown for another 2 weeks. Osteogenic differentiation was induced with DMEM supplemented with 10% fetal calf serum, 2 mmol/L l-glutamine, 100 nmol/L dexamethasone, 200 mmol/L L-ascorbic acid-2-phosphate, 10 mmol/L β-glycerophosphate, and 100 U/mL penicillin/streptomycin.^{14,15} To differentiate adipocytes, cells were grown in DMEM containing 10% fetal calf serum, 2 mmol/L l-glutamine, 1 mmol/L dexamethasone, 500 mmol/L 1-methyl-3-isobutylxanthine, 10 mg/mL insulin, and 100 U/mL penicillin/streptomycin.^{15,16} After 2 weeks, the cells were harvested and total RNA was isolated for the real-time polymerase chain reaction (PCR) analysis.

Immunofluorescence Staining

Mesenchymal stem cells were cultured on glass coverslips in 12-well plates prior to irradiation. After irradiation, cells were fixed with 4% formaldehyde for 15 minutes, permeabilized with 0.1%

Triton X-100 for 20 minutes, incubated with 0.2% bovine serum albumin for 1 hour, and stained with the indicated primary antibodies at 4°C overnight. On the next day, after 3 washes for 3 minutes each, the cells were treated with secondary antibodies for 1 hour at room temperature. Mounting medium for fluorescence with DAPI (Cat No: H-1200, Vector Laboratories, Inc. Burlingame, CA) was used to stain nuclear DNA. The antibodies used for immunofluorescence staining were anti-γ-H2AX and anti-Rad51 (1:200, Cell Signaling, Boston, Massachusetts). We assessed γH2AX and Rad51 foci as indicators of DNA double-strand breaks (DSBs). According to regular statistical standard for analyzing DNA damage repair protein foci,^{17,18} cells with >10 foci were counted as positive cells.

Cell Apoptosis Assay

For the cell apoptosis analysis, cells plated in 6-well plates were collected. An Annexin V-FITC Apoptosis Detection Kit was used to measure the number of apoptotic cells with flow cytometry. Briefly, cells were collected, washed with ice-cold phosphate-buffered saline (PBS) twice, and resuspended in binding buffer containing Annexin V and propidium iodide (PI) for 30 minutes at room temperature in the dark. After incubation, at least 10 000 cells were measured using a BD-FACS Aria flow cytometer.

Cell Cycle Analysis

Cells were harvested and washed with PBS. Then, cells were treated with methanol and resuspended in PI-staining buffer (50 µL/mL PI, RNase A) for 15 minutes at 37°C. The fluorescence intensity was analyzed using a flow cytometer.

Comet Assay

The Ad-MSCs, UC-MSCs, and G-MSCs were seeded in 6-well plates at a density of 1×10^5 cells/well. After exposure to 4- and 10-Gy irradiation, cells were collected and the cell density was adjusted to 1×10^5 to 1×10^6 with PBS. The comet assay was performed as described in a previous study.¹⁹ Briefly, the treated cell samples were prepared as single-cell suspensions. Thirty microliters of the cell suspension were mixed with 70 µL of low-melting-point agarose gel (Promega, Madison, Wisconsin). A drop of the mixture was added to a slide with agarose gel (Biowest, Nuaille, France) and then lysed. After the gel had solidified, it was placed in the pre-cooled pyrolysis solution and lysed for 2.5 hours at 4°C. After electrophoresis, the slides were neutralized, stained with ethidium bromide, and observed under a fluorescence microscope (ETLPS 90i; Nikon, Japan). The resulting images were analyzed using the Comet Assay Software Project (CASP, Wrocław University, Poland).

Real-Time PCR

Total RNA was isolated using Trizol reagent (Invitrogen, Carlsbad, CA) according to the manufacturer's specifications. Two

Table 1. Primer Sequences Used for Real-Time RT-PCR.

Gene	Forward Primer (5'→3')	Reverse Primer (5'→3')
Stat3	GGCATTGGGAAGTATTGTCG	GGTAGGCGCCTCAGTCGTATC
Nanog	CCCCTCCTCCCATCCCTC	GCTCCAACCATACTCCACCC
Oct4	GTATTCAGCCAAACGACCATC	GCTTCCTCCACCCACTTCT
Sox2	GGTTACCTCTTCTCCCACTCC	CCTCCCATTTCCTCGTTT
C-Myc	AATGAAAAGGCCCCCAAGGTATCC	GTCGTTTCCGCAACAAGTCCTCTTC
Bcl-2	CTGCACCTGACGCCCTTCACC	CACATGACCCACCGAACTCAAAGA
Cbfa1	ATGCTTCATTGCGCTCACAAAC	CCAAAAGAAGTTTTGCTGACATGG
Runx2	GCACAAACATGGCCAGATTCA	AAGCCATGGTGCCCGTTAG
PPAR- γ	GCTGTTATGGGTGAAACTCTG	ATAAGGTGGAGATGCAGGCTC
GAPDH	CTCTGATTTGGTCGTATTGGG	TGGAAGATGGTGATGGGATT

Abbreviations: RT-PCR, reverse transcriptase polymerase chain reaction; PPAR, peroxisome proliferator activated receptor.

micrograms of total RNA were reverse transcribed using a Reverse Transcription Kit (TIANGEN Biotech, Beijing, China), and real-time PCR was performed with the Opticon System (Bio-Rad, Hercules, USA) using a TransStart Green qPCR Super Mix Kit (TransGen Biotech, Beijing, China). The $2^{-\Delta\Delta Ct}$ method was used to assess the relative messenger RNA (mRNA) expression. Primers are listed in Table 1.

Western Blot Analysis

Cells were lysed in radioimmunoprecipitation assay buffer at 4°C for 20 to 30 minutes and centrifuged at $12\,000 \times g$ at 4°C for 15 minutes to obtain total protein lysates for immunoblot analyses. Equivalent amounts of proteins (20 μ g) were then separated by electrophoresis on 8% sodium dodecyl sulfate-polyacrylamide gel electrophoresis gels and transferred to polyvinyl difluoride membranes (EMD Millipore, Billerica, Massachusetts). After blocking, primary antibodies against Stat3, p-Stat3, Nanog, Oct4, c-Myc (Abcam, Cambridge, Massachusetts), and GAPDH (Santa Cruz Biotechnology Inc, Dallas, Texas) were separately incubated with the membranes at 4°C overnight. On the next day, after washing the membranes with Tris-buffered saline Tween 20, three times for 10 minutes each, secondary antibodies were incubated with the membranes at room temperature for 1 hour.

Statistical Analysis

Each experiment was performed at least 3 times, and all data were analyzed using GraphPad Prism software. Data were analyzed using 2-tailed Student *t* test or 2-way analysis of variance. A *P* value <0.05 was considered statistically significant.

Results

Mesenchymal Stem Cells Are Relatively Resistant to IR and Ad-MSCs Were the Most Resistant Cells

A cell proliferation assay was performed, and the morphology of cells treated with different doses of radiation was observed to examine the radiation responses of MSCs derived from adipose tissue, the umbilical cord, and gingival tissue. A significant difference in cell proliferation was not observed

between MSCs originating from different tissues (Figure 1B). All MSC samples presented a higher rate of cellular proliferation after exposure to 4 Gy of radiation than nonirradiated groups. The total numbers of UC-MSCs and G-MSCs, but not Ad-MSCs, decreased after irradiation at a dose of 10 Gy compared to 0 Gy. The Ad-MSCs presented a higher proliferation rate than UC-MSCs and G-MSCs, indicating that Ad-MSCs were the most resistant type among the 3 MSC samples (Figure 1A and B).

Irradiation Induces Higher Percentages of Apoptotic UC-MSCs and G-MSCs Than Ad-MSCs

Irradiation-induced apoptosis was measured in Ad-MSCs, UC-MSCs, and G-MSCs using flow cytometry. Consistent with previous reports, fewer irradiated MSCs underwent apoptosis.^{6,15} Irradiation of the 3 types of MSCs with doses of 4 and 10 Gy did not obviously increase the percentage of apoptotic cells, and thus the dose of 20 Gy was chosen to perform the MSC apoptosis assay. As shown in Figure 1, a small number of Ad-MSCs underwent apoptosis, while greater numbers of UC-MSCs and G-MSCs underwent apoptosis, with approximately 45% and 30%, respectively, of the total cells displaying apoptosis at 24 hours after irradiation.

Mesenchymal Stem Cells From Different Tissues Exhibit Heterogeneous Changes in the Cell Cycle After Irradiation

The cell cycle profiles of MSCs were analyzed after IR treatment using fluorescence-activated cell sorting. The influence of the tissue of origin on irradiation-induced effects on the cell cycle of MSCs was examined. At 1 day after irradiation, the percentages of cells in S phase decreased in the 3 types of MSCs, accompanied by an increase in the percentages of cells in either G1 or G2/M phase. Both UC-MSCs and G-MSCs exhibited a substantial decrease in the S phase population after irradiation. In contrast, irradiated Ad-MSCs did not display a significant decrease in the percentage of cells in S phase. A similar accumulation in G2/M phase was observed for 3 types of MSCs, while UC-MSCs exhibited

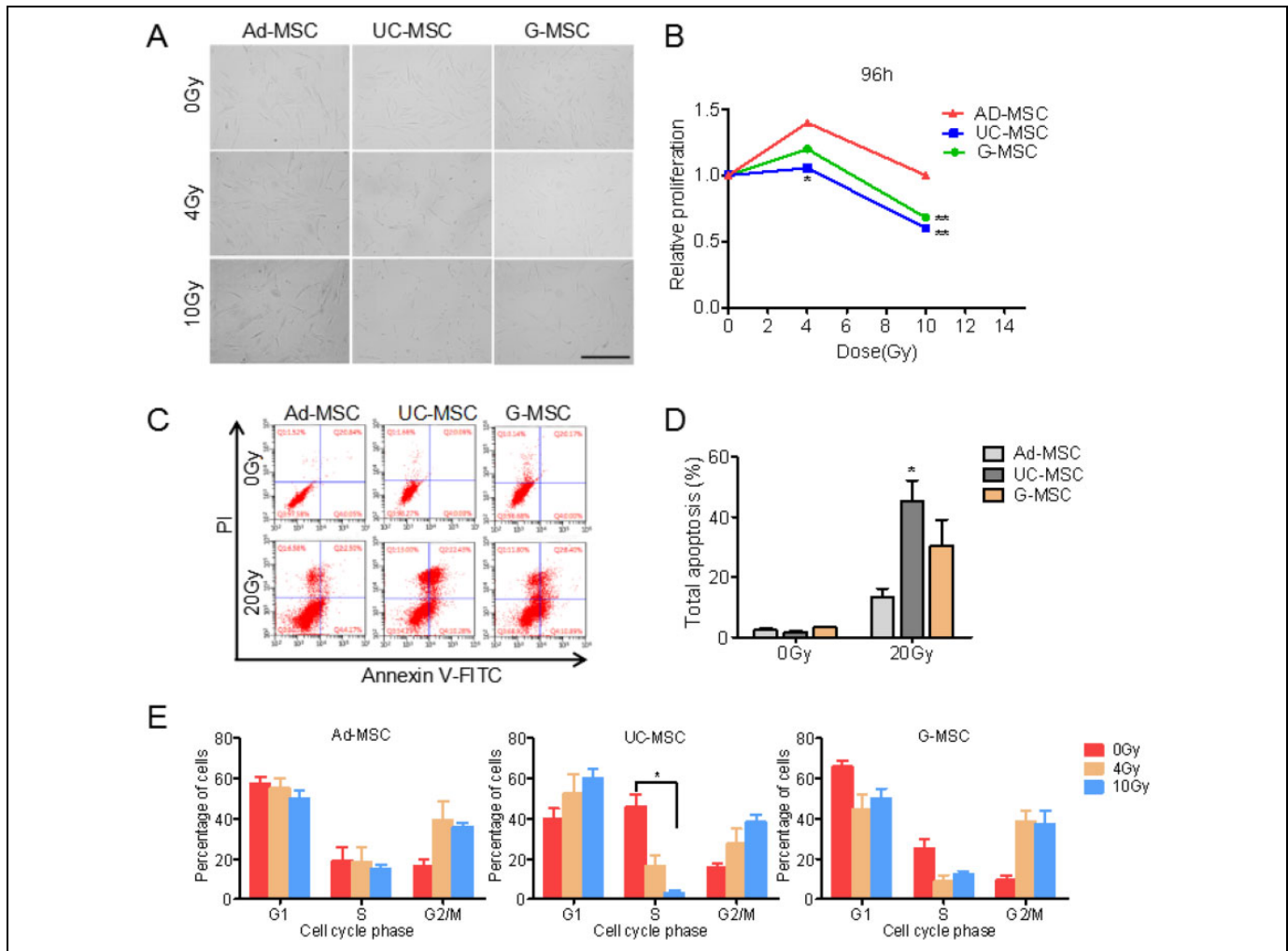


Figure 1. Morphology, proliferation rate, cell apoptosis, and cell cycle progression of mesenchymal stem cells (MSCs) after exposure to ionizing radiation. (A) Images of adipose tissue-derived MSCs (Ad-MSCs), umbilical cord-derived MSCs (UC-MSCs), and gingival tissue-derived MSCs (G-MSCs) after exposure to ionizing radiation; scale bar, 400 μ m. (B) Relative proliferation rates of Ad-MSCs, UC-MSCs, and G-MSCs after exposure to ionizing radiation. (C) and (D) Mesenchymal stem cells were exposed to 20 Gy of ionizing radiation. The percentage of apoptotic cells was assessed using fluorescence-activated cell sorting (FACS) 24 hours after irradiation. (E) Cells were exposed to 4 or 10 Gy of radiation, stained with propidium iodide (PI), and analyzed using FACS at 24 hours after irradiation. The proportions of cells in the different phases of the cell cycle were analyzed. Data are presented as the means \pm standard error (SD; error bars) from 3 independent experiments. * $P < 0.05$ and ** $P < 0.01$, $n = 3$.

irradiation-induced increases in the percentage of cells in G1 phase (Figure 1E).

Adipose-Derived MSCs Exhibit Less DNA Damage and More Efficient Repair Than UC-MSCs and G-MSCs After Irradiation

Irradiation induces DNA DSBs. The γ -H2AX and Rad51 foci were measured using immunofluorescence staining and microscopy to further assess the ability of MSCs from different tissues to efficiently repair DNA DSBs. γ -H2AX plays a key role in recruiting repair proteins to the sites of DNA DSBs.^{20,21} Irradiation with 4 or 10 Gy resulted in large numbers of initial strand breaks at 1 hour after irradiation. Greater

numbers of γ -H2AX and Rad51 foci were detected in the 3 types of MSCs at 1 hour post-irradiation. By 24 hours after IR, the significant decrease in γ -H2AX and Rad51 foci was more evident in Ad-MSCs than in both UC-MSCs and G-MSCs, suggesting that Ad-MSCs may possess a greater capacity for repairing IR-induced DNA damage than UC-MSCs and G-MSCs (Figure 2).

DNA damage was further investigated using the comet assay. As shown in Figure 3, the irradiated Ad-MSCs exhibited a lower percentage of tail DNA and olive tail moment than UC-MSCs and G-MSCs, indicating that Ad-MSCs were more resistant to radiation than UC-MSCs and G-MSCs. Based on these results, Ad-MSCs may possess a greater capacity to repair IR-induced DNA DSBs than UC-MSCs and

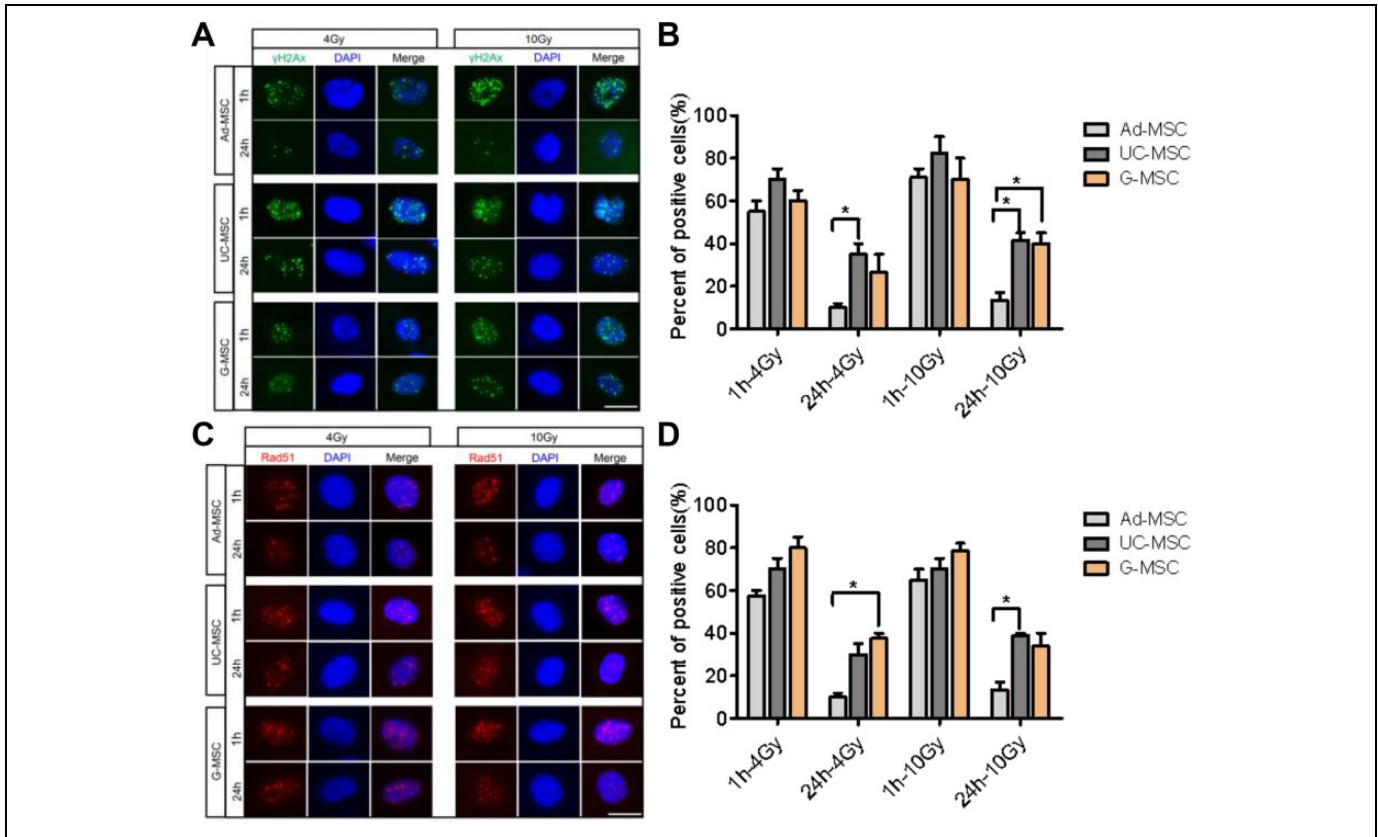


Figure 2. Mesenchymal stem cells (MSCs) repair DNA damage. (A) Representative images of immunofluorescence staining for 4',6-diamidino-2-phenylindole (DAPI) and γ -H2AX (green) in adipose tissue-derived MSCs (Ad-MSCs), umbilical cord-derived MSCs (UC-MSCs), and gingival tissue-derived MSCs (G-MSCs) at 1 and 24 hours after irradiation with 4 or 10 Gy. (B) Histogram showing the percentage of cells with >10 γ -H2AX nuclear foci. The data are presented as the means of 3 independent experiments \pm standard error of the mean (SEM); * $P < 0.05$). (C) Representative images of immunofluorescence staining for DAPI and Rad51 (red) in Ad-MSCs, UC-MSCs, and G-MSCs at 1 and 24 hours after irradiation with 4 or 10 Gy; scale bar, 25 μ m; * $P < 0.05$, $n = 3$. (D) Histogram showing the percentage of cells with >10 Rad51 nuclear foci. The data are presented as the means of 3 independent experiments \pm SEM (* $P < 0.05$).

G-MSCs, which likely contributes to their greater ability to survive after exposure to IR.

Irradiated Ad-MSCs Maintain the Expression of Stem Cell-Related Genes to a Greater Extent Than UC-MSCs and G-MSCs

Activation of the Stat3 pathway has been shown to enhance tumor stem-like cell self-renewal and further promote tumor invasion and radioresistance.²²⁻²⁴ Stem cells are more resistant to radiation than tissue cells due to their self-renewal ability. Stat3 has multiple targets, including Nanog, Oct4, Sox2, c-Myc, and Bcl-2.^{25,26} We examined the mRNA and protein levels of these genes to investigate whether the greater radiation resistance capacity of Ad-MSCs was attributed to the activation of the Stat3 pathway. After exposure to IR, the expression of stemness-related genes was significantly upregulated in irradiated Ad-MSCs; however, obvious differences were not observed between irradiated UC-MSCs, G-MSCs, and nonirradiated cells (Figure 4A). Gene expression in

irradiated Ad-MSCs was higher than in irradiated UC-MSCs and G-MSCs.

Western blot analyses were performed to assess the activation of key proteins involved in Stat3 signaling. High levels of phosphorylated Stat3 were observed in Ad-MSCs after exposure to 4 Gy of radiation; however, the levels were substantially reduced in UC-MSCs and G-MSCs, suggesting a continuous activation of Stat3 signaling in Ad-MSCs. Irradiated Ad-MSCs displayed higher levels of Nanog, Oct4, and c-Myc than UC-MSCs and G-MSCs (Figure 4C).

Mesenchymal Stem Cells Retain Their Differentiation Potential After Irradiation Irrespective of Their Tissue of Origin

In order to better characterize different tissue of MSCs, we next aimed to determine their level of differentiation potential. The ability for differentiation along the adipogenic and osteogenic lineages is a hallmark of MSCs. Osteogenic and adipogenic differentiation were assessed by determination of osteogenesis marker Cbfa1, Runx2, and adipogenic marker peroxisome

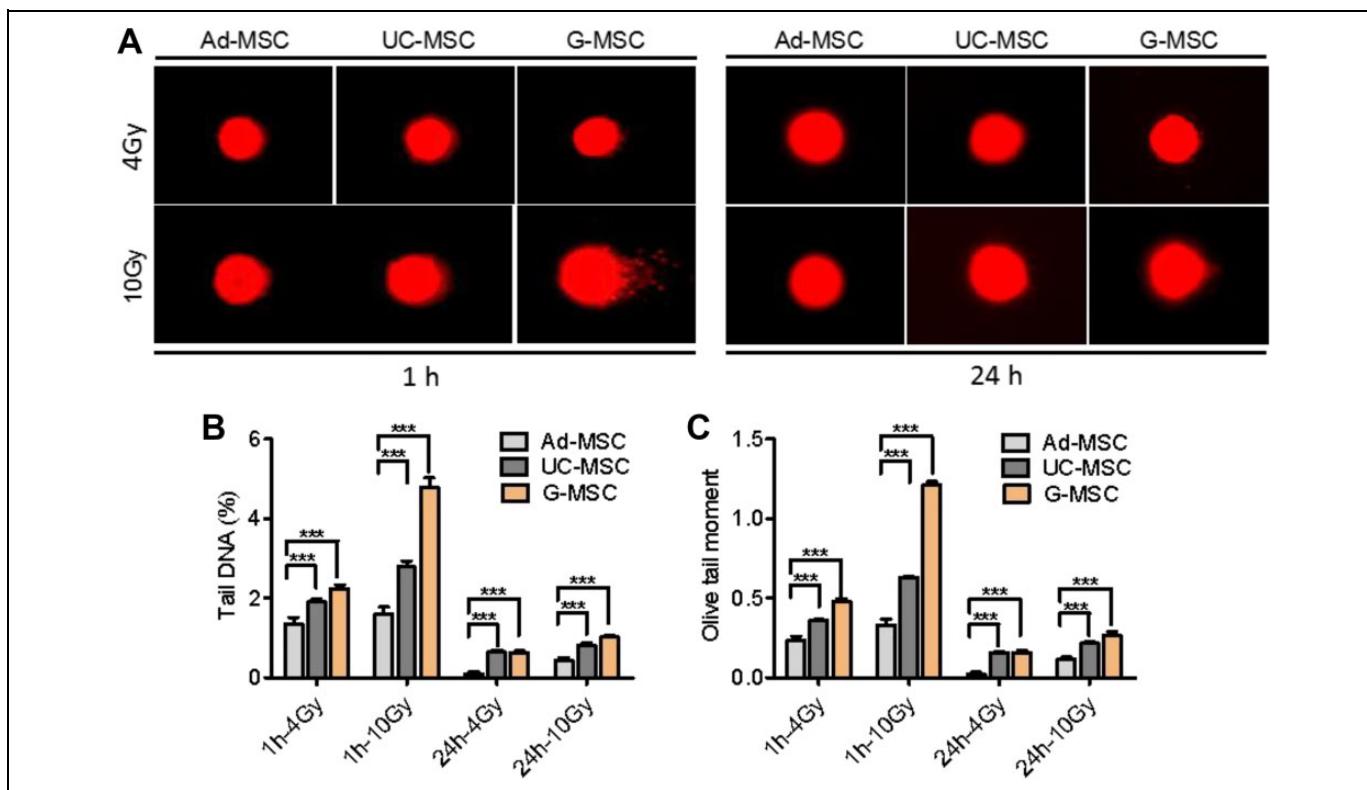


Figure 3. Mesenchymal stem cells (MSCs) repair DNA double-strand breaks. (A) Representative images of the comet assay using adipose tissue-derived MSCs (Ad-MSCs), umbilical cord-derived MSCs (UC-MSCs), and gingival tissue-derived MSCs (G-MSCs) at 1 and 24 hours after irradiation with 4 or 10 Gy of ionizing radiation (IR). (B) Histogram showing the percentage of tail DNA. (C) Histogram showing the olive tail moment. The quantitative analysis of DNA strand break outputs is presented as the means of 3 independent experiments \pm standard error of the mean (SEM; *** $P < 0.001$).

proliferator activated receptor. It was observed that all MSC types possessed capacity of osteogenic and adipogenic differentiation, where Ad-MSCs showed pronounced osteogenesis in comparison to other MSCs, and UC-MSCs demonstrated increases in induced adipogenic differentiation (Figure 4B). However, there was no significant or dose-dependent reduction in the potential for adipogenic or osteogenic differentiation in any of the MSC specimens after irradiation.

Discussion

The effect of IR on MSCs has been extensively explored. Mesenchymal stem cells are known to be radioresistant. However, various publications reported a strong heterogeneity of MSCs from different tissues, which was a major challenge for establishing MSC-based therapeutic approaches to treat radiation injury. The influence of MSC tissue heterogeneity on the radiation responses of these cells is largely unknown. Here, irradiated MSCs from 3 sources exhibited different responses to IR.

Our study examined the effects of radiation on MSCs originating from different tissues and revealed that MSCs from adipose tissue exhibited stronger radioresistance than MSCs from the umbilical cord or gingival tissue. In our study, we

determined radiation-induced changes in cell proliferation, apoptosis, cell cycle progression, DNA damage and repair, and expression patterns of self-renewal-related genes using MSCs from these 3 sources. The responses of Ad-MSCs to radiation differed from UC-MSCs and G-MSCs. Adipose-derived MSCs were highly proliferative, and fewer cells underwent apoptosis upon exposure to the same dose of radiation (Figure 1B and D). Moreover, an obvious difference in the percentage of irradiated Ad-MSCs and nonirradiated Ad-MSCs in S phase was not observed. However, fewer irradiated UC-MSCs and G-MSCs were in S phase compared to the 0 Gy condition (Figure 1E). In a previous study, twice the number of radioresistant cells was in S phase than the more sensitive cell line.^{27,28} This finding may potentially explain the increased radioresistance of Ad-MSCs compared to UC-MSCs and G-MSCs.

Ionizing radiation induces high levels of genotoxic stress due to the production of reactive oxygen species and a wide range of genomic lesions, including DNA DSBs.²⁹ The response to DNA DSBs is characterized by the formation of γ -H2AX and Rad51 foci,³⁰ which are DNA damage and repair markers, respectively.⁹ Levels of γ -H2AX and Rad51 were significantly decreased in irradiated Ad-MSCs at 24 hours after exposure to IR compared with UC-MSCs and G-MSCs, showing a rapid DNA repair activity (Figure 2). Based on the result from the comet assay,

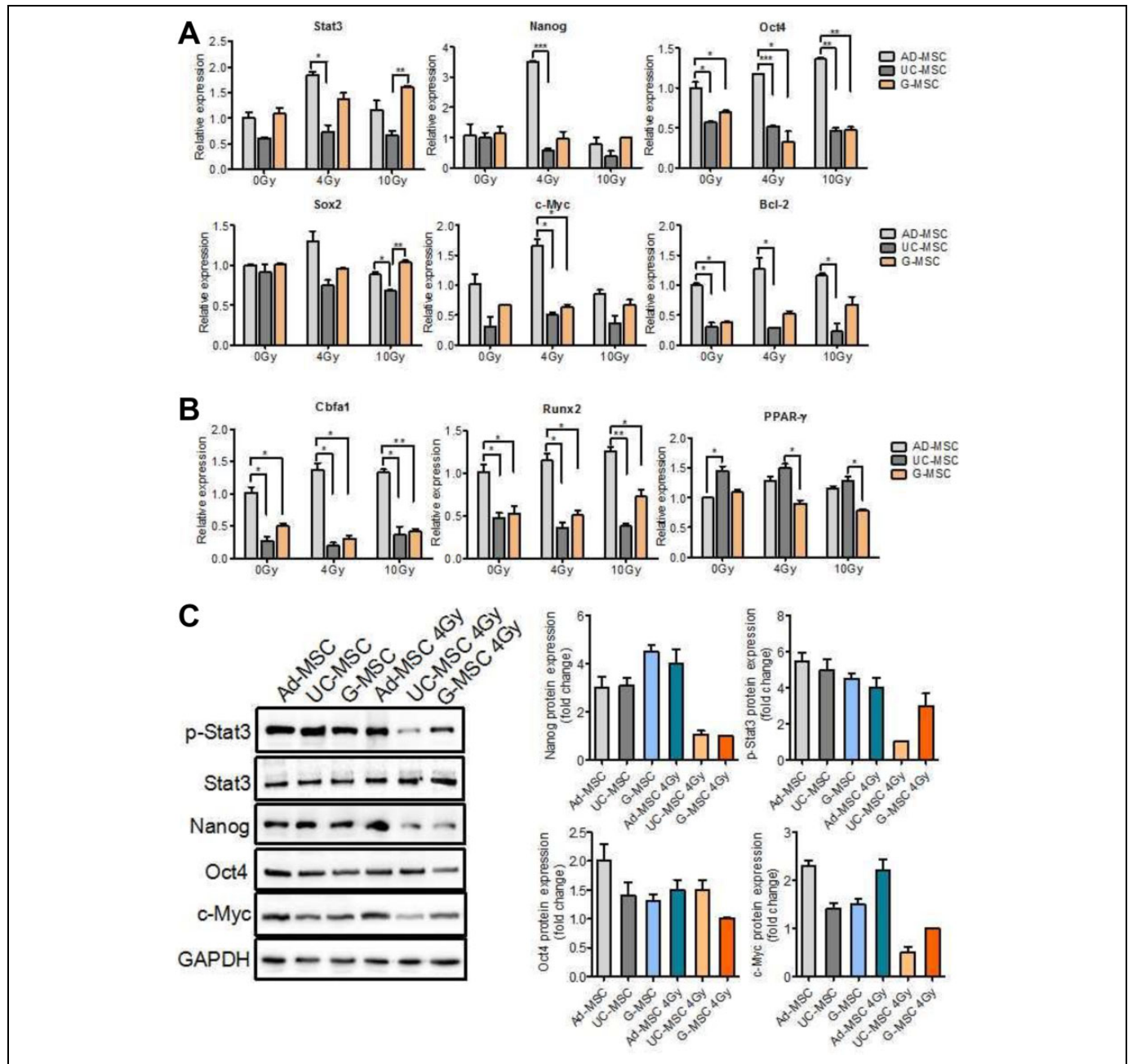


Figure 4. Stat3, its target genes, and the differentiation genes' expression in MSCs. (A) Polymerase chain reaction (PCR) analysis of the expression of Stat3 and its related genes. Cells were harvested at 48 hours after irradiation. (B) Polymerase chain reaction analysis of the expression of differentiation genes. Osteogenic marker Cbfa1, Runx2, and adipogenic marker PPAR- γ . Cells were harvested after differentiation culture. (C) Western blot analyses of different proteins involved in Stat3 signaling. Cells were harvested at 48 hours after irradiation. The data are presented as the means of 3 independent experiments \pm standard error of the mean (SEM; * $P < 0.05$, ** $P < 0.01$, and *** $P < 0.001$).

Ad-MSCs had a lower level of radiation-induced DNA damage than UC-MSCs and G-MSCs (Figure 3). Our study has identified mechanisms that potentially mediate radioresistance in Ad-MSCs, including a low IR-induced apoptotic response and the rapid formation of γ -H2AX and Rad51 foci for robust DSB repair activation. The self-renewal capability of stem cells is responsible for the radiation resistance.⁹ The self-renewal associated marker Stat3 is well known to function as an anti-apoptotic

factor, especially in numerous malignancies. Lacking Stat3 is more sensitive to oxidative stress, and a key feature of oxidative stress involves activation of the DNA damage pathway.³¹ Therefore, the Stat3 may be considered as a potential biomarker of radiation resistance. We measured the expression of Stat3 and its downstream genes. Irradiated Ad-MSCs exhibited higher expression of these genes than irradiated UC-MSCs and G-MSCs (Figure 4).

In conclusion, MSCs from adipose tissue exhibit stronger radioresistance due to their efficient repair of irradiation-induced DNA damage, corresponding to low levels of apoptosis and up-regulated expression of stemness-related genes. These findings improve our understanding of the radiation-induced responses of MSCs and may lead to the development of better strategies for irradiation-induced tissue damage and cancer therapy.

Authors' Note

Ningning He, Changyan Xiao, and Yuxiao Sun contributed equally to this work.


Declaration of Conflicting Interests


The author(s) declared no potential conflicts of interest with respect to the research, authorship, and/or publication of this article.


Funding

The author(s) disclosed receipt of the following financial support for the research, authorship, and/or publication of this article: This study was supported by the National Natural Science Foundation of China (No.31670859, 31800703), Natural Science Foundation of Tianjin (No. 18JCQNJC12300, 18JCYBJC26800), CAMS Innovation Fund for Medical Science (No.2017-I2M-1-016, 2016-I2M-1-017), the Fundamental Research Funds for the Central Universities (No.3332019006), China Postdoctoral Science Foundation (No.2018M630106), the Fundamental Research Funds for the Central Universities (10023201601602).

ORCID iD

Ningning He  <https://orcid.org/0000-0002-2360-6203>

Yuxiao Sun  <https://orcid.org/0000-0001-7019-5833>

Qiang Liu  <https://orcid.org/0000-0002-7668-6868>

References

- Zhang J, Lv S, Liu X, Song B, Shi L. Umbilical cord mesenchymal stem cell treatment for Crohn's disease: a randomized controlled clinical trial. *Gut Liver*. 2018;12(1):73-78.
- Jackson WM, Nesti LJ, Tuan RS. Mesenchymal stem cell therapy for attenuation of scar formation during wound healing. *Stem Cell Res Ther*. 2012;3(3):20.
- Kim HJ, Seo SW, Chang JW, et al. Stereotactic brain injection of human umbilical cord blood mesenchymal stem cells in patients with Alzheimer's disease dementia: a phase I clinical trial. *Alzheimers Dement*. 2015;1(2):95-102.
- Li R, Li XM, Chen JR. Clinical efficacy and safety of autologous stem cell transplantation for patients with ST-segment elevation myocardial infarction. *Ther Clin Risk Manag*. 2016;12:1171-1189.
- Nedeau AE, Bauer RJ, Gallagher K, Chen H, Liu ZJ, Velazquez OC. A CXCL5- and bFGF-dependent effect of PDGF-B-activated fibroblasts in promoting trafficking and differentiation of bone marrow-derived mesenchymal stem cells. *Exp Cell Res*. 2008;314(11-12):2176-2186.
- Ruhle A, Xia O, Perez RL, et al. The radiation resistance of human multipotent mesenchymal stromal cells is independent of their tissue of origin. *Int J Radiat Oncol Biol Phys*. 2018;100(5):1259-1269.
- Valle-Prieto A, Conget PA. Human mesenchymal stem cells efficiently manage oxidative stress. *Stem Cells Dev*. 2010;19(12):1885-1893.
- Chen MF, Lin CT, Chen WC, et al. The sensitivity of human mesenchymal stem cells to ionizing radiation. *Int J Radiat Oncol Biol Phys*. 2006;66(1):244-253.
- Maria OM, Kumala S, Heravi M, Syme A, Eliopoulos N, Muanza T. Adipose mesenchymal stromal cells response to ionizing radiation. *Cytotherapy*. 2016;18(3):384-401.
- Chang P, Qu Y, Liu Y, et al. Multi-therapeutic effects of human adipose-derived mesenchymal stem cells on radiation-induced intestinal injury. *Cell Death Dis*. 2013;4:e685.
- Semont A, Mouisseddine M, Francois A, et al. Mesenchymal stem cells improve small intestinal integrity through regulation of endogenous epithelial cell homeostasis. *Cell Death Differ*. 2010;17(6):952-961.
- Semont A, Francois S, Mouisseddine M, et al. Mesenchymal stem cells increase self-renewal of small intestinal epithelium and accelerate structural recovery after radiation injury. *Adv Exp Med Biol*. 2006;585:19-30.
- Yang ZX, Han ZB, Ji YR, et al. CD106 identifies a subpopulation of mesenchymal stem cells with unique immunomodulatory properties. *PLoS One*. 2013;8(3):e59354.
- Maes C, Coenegrachts L, Stockmans I, et al. Placental growth factor mediates mesenchymal cell development, cartilage turnover, and bone remodeling during fracture repair. *J Clin Invest*. 2006;116(5):1230-1242.
- Nicolay NH, Sommer E, Lopez R, et al. Mesenchymal stem cells retain their defining stem cell characteristics after exposure to ionizing radiation. *Int J Radiat Oncol Biol Phys*. 2013;87(5):1171-1178.
- Pittenger MF, Mackay AM, Beck SC, et al. Multilineage potential of adult human mesenchymal stem cells. *Science*. 1999;284(5411):143-147.
- Patel AG, Sarkaria JNK, Aufmann SH. Nonhomologous end joining drives poly(ADP-ribose) polymerase (PARP) inhibitor lethality in homologous recombination-deficient cells. *Proc Natl Acad Sci U S A*. 2011;108(8):3406-3411.
- Raderschall E, Golub EI, Haaf T. Nuclear foci of mammalian recombination proteins are located at single-stranded DNA regions formed after DNA damage. *Proc Natl Acad Sci U S A*. 1999;96(5):1921-1926.
- Li J, Wang Y, Du L, et al. Nested PCR for mtDNA-4977-bp deletion and comet assay for DNA damage - a combined method for radiosensitivity evaluation of tumor cells. *Oncol Lett*. 2014;7(4):1083-1087.
- Rogakou EP, Pilch DR, Orr AH, Ivanova VS, Bonner WM. DNA double-stranded breaks induce histone H2AX phosphorylation on serine 139. *J Biol Chem*. 1998;273(10):5858-5868.
- Hou J, Han ZP, Jing YY, et al. Autophagy prevents irradiation injury and maintains stemness through decreasing ROS generation in mesenchymal stem cells. *Cell Death Dis*. 2013;4:e844. doi:10.1038/cddis.2013.338.

22. Lin JC, Tsai JT, Chao TY, Ma HI, Liu WH. The STAT3/Slug Axis Enhances Radiation-Induced Tumor Invasion and Cancer Stem-like Properties in Radioresistant Glioblastoma. *Cancers*. 2018;10(12):E512.
23. Lee JH, Choi SI, Kim RK, Cho EW, Kim IG. Tescalcin/c-Src/IGF1Rbeta-mediated STAT3 activation enhances cancer stemness and radioresistant properties through ALDH1. *Sci Rep*. 2018;8(1):10711. doi: 10.1038/s41598-018-29142-x.
24. Almiron Bonnin DA, Havrda MC, Lee MC, et al. Secretion-mediated STAT3 activation promotes self-renewal of glioma stem-like cells during hypoxia. *Oncogene*. 2018;37(8):1107-1118.
25. Bourillot PY, Aksoy I, Schreiber V, et al. Novel STAT3 target genes exert distinct roles in the inhibition of mesoderm and endoderm differentiation in cooperation with Nanog. *Stem Cells*. 2009;27(8):1760-1771.
26. Yang J, Van Oosten AL, Theunissen TW, Guo G, Silva JC, Smith A. Stat3 activation is limiting for reprogramming to ground state pluripotency. *Cell Stem Cell*. 2010;7(3):319-328.
27. Quiet CA, Weichselbaum RR, Grdina DJ. Variation in radiation sensitivity during the cell cycle of two human squamous cell carcinomas. *Int J Radiat Oncol Biol Phys*. 1991;20(4):733-738.
28. Islam MS, Stemig ME, Takahashi Y, Hui SK. Radiation response of mesenchymal stem cells derived from bone marrow and human pluripotent stem cells. *J Radiat Res*. 2015;56(2):269-277.
29. Sugrue T, Brown JA, Lowndes NF, Ceredig R. Multiple facets of the DNA damage response contribute to the radioresistance of mouse mesenchymal stromal cell lines. *Stem Cells*. 2013;31(1):137-145.
30. Fernandez-Capetillo O, Lee A, Nussenzweig M, Nussenzweig A. H2AX: the histone guardian of the genome. *DNA Repair*. 2004;3(8-9):959-967.
31. Barry SP, Townsend PA, Knight RA, Scarabelli TM, Latchman DS, Stephanou A. STAT3 modulates the DNA damage response pathway. *Int J Exp Pathol*. 2010;91(6):506-514.